International Journal of Multidisciplinary Research and Publications
ISSN (Online): 2581-6187

Design and Performance Analysis of an Asymmetrical Propeller for Noise Reduction

Joseph Nikolai Alfonso[1], Zeidred Bago[2], Chleyde Dexier Danguilan[3], Jay Christian Leria[4], Von Harl Rian Madjos[5], John Raven Ramirez[6], Artzache Yhazee Solis[7], Mycka Jiemel Villamor[8]

[1,2,3,4,5,6,7,8]Department of Aeronautical Engineering, PATTS College of Aeronautics, Parañaque City, Metro Manila, Philippines
[1]josephnikolai.alfonso@gmail.com, [2]zeidred22@gmail.com, [3]chleydedexierdanguilan@gmail.com, [4]jaycleria@gmail.com, [5]vonharlrian.madjos@gmail.com, [6]ramirezjohnraven664@gmail.com, [7]artzacheyhazee.solis@gmail.com, [8]villamormycka@gmail.com

Abstract*—Rotorcraft and small unmanned aerial vehicles continue to face strong public and regulatory pressure to operate more quietly, especially in low-altitude urban airspace where blade-passing tones dominate the perceived signature. This study examined whether asymmetrical blade spacing can deliver such a reduction without sacrificing propulsive efficiency. Three two-bladed asymmetrical propellers with Blade Sector Angles (BSA) of 30°, 60° and 90° were designed in Autodesk Fusion 360 around a NACA 4412 section selected from a comparative XFLR5 evaluation, then fabricated by Fused Deposition Modeling on a Creality Ender 3 V3 KE printer using ASA filament. A symmetrical two-bladed propeller of the same diameter served as the control. Sound pressure level, thrust, rotational speed and electrical power were recorded at 2,000, 3,000 and 4,000 RPM with fifteen replications per condition, and the data were processed through Shapiro–Wilk normality, Levene homogeneity, Student or Welch t-tests, and Cohen's d. The conventional propeller remained the quietest configuration at every tested RPM, but the 90° BSA propeller produced a higher mean thrust-to-power ratio than the conventional design at 2,000 and 3,000 RPM while remaining the quietest of the asymmetrical variants. The findings expose a measurable trade-off between aeroacoustics and propulsive performance that depends jointly on blade spacing and operating speed.*

***Keywords*—** *Asymmetrical propeller: aeroacoustics: blade sector angle: drone noise: fused deposition modelling: NACA 4412: thrust-to-power ratio: UAV propulsion.*

I. Introduction

The proliferation of small unmanned aerial vehicles (UAVs) for last-mile delivery, aerial photography, surveying and emergency response has placed propeller noise at the center of community-acceptance debates. Acoustic surveys of multirotor platforms in hover routinely report A-weighted sound pressure levels between 70 and 80 dBA at short observation distances, with strong tonal content at the blade-passing frequency that listeners consistently judge as more annoying than equivalently loud broadband noise [1], [2]. The annoyance penalty associated with this tonal character is severe enough that future certification frameworks for urban air mobility are expected to constrain it directly rather than relying on overall level alone [3].

Conventional symmetrical propellers, in which the blades are equally spaced around the hub, concentrate aerodynamic loading into a narrow harmonic series whose fundamental coincides with the blade-passing frequency. This concentration is acoustically unfavorable: it produces a sharp tone at a frequency to which the human ear is highly sensitive, and small increases in rotational speed translate directly into perceptible changes in pitch [4], [5]. A growing body of analytical and computational work has therefore proposed redistributing the blades around the hub, so that the periodic source becomes a sum of weaker, frequency-spread components [6]–[8]. Such asymmetrical or unevenly spaced rotors have been studied for full-scale helicopters, ducted fans and compound rotorcraft, but experimental evidence on small two-bladed UAV propellers, manufactured with the additive-manufacturing techniques common in academic and hobbyist settings, remains sparse and largely qualitative [9], [10].

The handful of published experiments on asymmetrical small-scale propellers report contradictory outcomes. Some authors observe a measurable reduction of the dominant tone at the cost of additional broadband noise [7], [11], while others find no statistically reliable improvement once measurement uncertainty is accounted for [12]. Differences in airfoil section, hub geometry, manufacturing method and acoustic environment make direct comparison difficult, and few studies pair acoustic results with rigorous propulsive-efficiency measurements at the same operating points. The result is a gap that this study set out to address: whether a controlled variation of the Blade Sector Angle (BSA) of a two-bladed, NACA 4412-based, FDM-printed propeller can simultaneously alter its sound pressure level and its thrust-to-power ratio at operating speeds typical of small consumer drones.

To examine that question, three asymmetrical propellers were modeled with BSA values of 30°, 60° and 90° and benchmarked against a symmetrical two-bladed control of identical diameter, airfoil and blade angle. All four prototypes were printed under the same parameters on a Creality Ender 3 V3 KE using ASA filament and tested on a custom thrust rig instrumented with an Audio-Technica AT2020 condenser microphone, a digital tachometer and a brushless-motor power analyzer. Sound pressure level, thrust, rotational speed and electrical power were measured at 2,000, 3,000 and 4,000 RPM with fifteen replications per condition. The data were screened with Shapiro–Wilk and Levene tests and compared

Joseph Nikolai Alfonso, Zeidred Bago, Chleyde Dexier Danguilan, Jay Christian Leria, Von Harl Rian Madjos, John Raven Ramirez, Artzache Yhazee Solis, Mycka Jiemel Villamor, "Design and Performance Analysis of an Asymmetrical Propeller for Noise Reduction," International Journal of Multidisciplinary Research and Publications (IJMRAP), Volume 9, Issue 1, pp. 1041–1051, June 2026.

by Student or Welch t-tests; effect magnitudes were reported through Cohen's d, and qualitative interview data from nine researchers and three industry experts were synthesized by reflexive thematic analysis.

The contribution of the present work is therefore threefold. It supplies a fully documented design–manufacture–test pipeline for asymmetrical small UAV propellers that can be replicated with low-cost equipment. It quantifies, with statistical rigor and a sample size large enough to support inferential testing, the acoustic and propulsive consequences of a controlled BSA sweep on a single airfoil family. And it positions those measurements against existing analytical predictions to clarify which expectations from the literature transfer to the small-rotor regime and which do not. The remainder of the paper is organized as follows. Section II reviews related work on propeller noise, asymmetrical blade spacing and additive manufacturing of small rotors. Section III details the design, fabrication, instrumentation and statistical methods. Section IV presents the noise and thrust-to-power results, their statistical comparisons against the conventional baseline, and a thematic synthesis of the qualitative interviews. Section V draws the conclusions, acknowledges the limitations of the experimental setup and outlines future research.

II. Literature Review

A. Sources of Propeller Noise in Small Rotorcraft

Propeller noise is conventionally decomposed into tonal and broadband components. Tonal noise arises from the periodic loading and thickness pulses of each blade, producing harmonics of the blade-passing frequency, while broadband noise originates in turbulence ingestion, blade self-noise and tip-vortex interactions [4], [13]. The first two blade-passing harmonics usually define the perceived sound character and dominate the spectrum for small two-bladed rotors operated at less than 5,000 RPM [1], [14]. Casalino and Nardari [13] showed through high-fidelity Lattice-Boltzmann simulations that the tonal peaks of a small drone rotor remain narrow and energetic even when blade Mach numbers stay well below transonic values, which makes any geometric measure that smears those peaks attractive from an annoyance perspective [3].

Empirical studies on consumer-class quadcopters report A-weighted SPL in the 70–80 dBA band at short ranges, with tonal prominences exceeding the surrounding broadband floor by 10–15 dB at the blade-passing frequency [2], [15]. Yang et al. [16] further demonstrated that subtle changes in blade twist, sweep and tip geometry can shift the balance between tonal and broadband contributions without large penalties in thrust, suggesting that rotor noise is sensitive to detailed geometric choices that are often treated as secondary.

B. Asymmetrical and Unevenly Spaced Blades

The idea of distributing the blades unevenly around the hub to disperse tonal energy across a wider frequency band predates UAV applications; it has been studied for cooling fans, helicopter rotors and aircraft propellers since the 1970s [4]. Modern computational work confirms the basic mechanism: when the azimuthal spacing of the blades departs from uniform, the spectrum loses its single dominant harmonic and gains a comb of weaker components whose perceived loudness, weighted with psychoacoustic metrics, is generally lower [6], [17].

Recent work targeting small UAV rotors has produced more nuanced findings. Usov et al. [7] tested asymmetric two-bladed propellers in a static rig and observed measurable tonal-noise reduction at the cost of additional broadband content. Koning et al. [8] reported similar trends from a hover-stand campaign and attributed residual gains to careful matching of blade-spacing angle and tip Mach number. Litherland et al. [11] focused on chord and camber asymmetry rather than azimuthal asymmetry and found that aerodynamically driven blade-loading variation can also redistribute acoustic energy. Shpak and Trostinsky [18] cautioned that some published reductions vanish once tip-loss and motor-electromagnetic noise are properly subtracted, underlining the sensitivity of these experiments to test setup.

C. Airfoil Selection for Small UAV Propeller Blades

Airfoil choice influences both lift-to-drag performance and the spectral character of the radiated noise. The NACA four-digit family remains popular for small rotors because the family has been characterized across a wide Reynolds-number range and is easy to manufacture by FDM. Vijayanandh et al. [19] compared several four- and five-digit sections for sub-100,000 Reynolds-number UAV propellers and found NACA 4412 to balance lift coefficient, lift-to-drag ratio and structural depth more favorably than thinner sections such as NACA 2410. Rahmat [20] reported that thicker leading edges suppress small-scale separation bubbles that contribute to broadband self-noise, while McKay et al. [1] linked blade-section choice to changes in tip-vortex strength and therefore to tonal-noise amplitude.

Bio-inspired airfoil modifications have also drawn attention. Noda et al. [21] examined leading-edge serrations inspired by owl wings and reported a 2–4 dB drop in mid-frequency noise on small UAV blades. While such modifications were beyond the scope of the present study, they exemplify the broader trend of treating airfoil geometry as an aeroacoustics design variable rather than a purely aerodynamic one [5], [22].

D. Additive Manufacturing of Small Rotor Prototypes

Fused Deposition Modeling has become the default fabrication route for academic propeller research because it is inexpensive, repeatable and tolerant to geometric experimentation. Selig and McGranahan [23] established that FDM-printed propellers can reproduce the aerodynamic performance of injection-molded counterparts to within a few percent provided that infill density, layer height and post-processing are controlled. ASA filament, used in this study, has gradually replaced PLA for outdoor and high-temperature work because of its higher glass-transition temperature and resistance to ultraviolet degradation [24].

Two recurrent practical issues complicate FDM rotor work. First, the additional mass from infill and supports shifts the blade's center of mass. This is especially troublesome for

Joseph Nikolai Alfonso, Zeidred Bago, Chleyde Dexier Danguilan, Jay Christian Leria, Von Harl Rian Madjos, John Raven Ramirez, Artzache Yhazee Solis, Mycka Jiemel Villamor, "Design and Performance Analysis of an Asymmetrical Propeller for Noise Reduction," International Journal of Multidisciplinary Research and Publications (IJMRAP), Volume 9, Issue 1, pp. 1041–1051, June 2026.

asymmetrical designs since they already have unbalanced inertia distributions [12]. Second, the surface roughness left by layer lines alters boundary-layer behavior at low Reynolds numbers and can introduce additional broadband noise that masks any tonal reduction obtained through blade redistribution [22], [25]. Both issues motivated the post-processing protocol adopted in this study, including 1000-grit sanding and a precisely placed 5-gram counterweight.

E. Measurement Methods for Acoustic and Propulsive Performance

Acoustic characterization of small rotors is most commonly performed indoors with a single condenser microphone at a distance of 0.1–1.0 m, sampled at audio rates and post-processed through narrowband and one-third-octave analysis [1], [26]. The Audio-Technica AT2020 used here has been adopted in earlier UAV studies because of its flat 20–20,000 Hz response and modest cost [27]. Open-air or anechoic facilities yield cleaner spectra but are not always available; semi-anechoic enclosures and low-reverberation rooms can achieve repeatable measurements provided that the propeller is mounted at a sufficient distance from acoustically reflective surfaces [3], [13].

Thrust and power measurements typically rely on load-cell or kitchen-scale rigs coupled with brushless motors driven at programmed RPM steps [12], [16]. The thrust-to-power ratio (T/P, kg/kW) collapses propulsive performance into a single figure of merit comparable to figure-of-merit definitions used in helicopter rotor analysis [11]. RPM is most reliably read with optical tachometers triggered by reflective tape, with the laser sensor placed at a distance that avoids aerodynamic perturbation [1], [25].

F. Statistical Treatment in Small-Sample Aeroacoustic Studies

Small-rotor experiments commonly suffer from limited replication, leading to under-powered comparisons and inflated effect-size estimates. Karch [28] and West [29] argue that even modest replication budgets can support robust inference if normality and homogeneity-of-variance assumptions are tested before parametric comparisons are applied, and if non-parametric or Welch-corrected alternatives are used when these assumptions fail. Cohen's d should accompany p-values to guard against the inflation of statistical significance that follows from very small measurement noise on instruments such as digital SPL meters [30].

Qualitative methods complement quantitative measurements when the research question concerns perceived noise. Naeem et al. [31] articulated a six-phase reflexive thematic analysis procedure that has been used in transport-noise research to surface the descriptors that listeners spontaneously apply to drone sounds. Lotinga et al. [3] integrated such qualitative testimony with measured spectra to argue that descriptive labels such as 'sharp', 'intrusive' and 'buzzing' map onto identifiable spectral signatures that engineers can target.

G. Synthesis and Identified Gap

Across the reviewed literature, three observations recur. First, asymmetrical blade spacing is theoretically attractive but its empirical benefits on small two-bladed UAV rotors are mixed and depend on operating speed [7], [8], [18]. Second, NACA 4412 remains a defensible airfoil baseline for sub-100,000 Reynolds-number propellers when both aerodynamic efficiency and fabrication tolerance are weighed [19], [20]. Third, no published study to date combines a controlled BSA sweep on a single airfoil and a single FDM workflow with a statistical sample large enough to support inferential testing of both noise and thrust-to-power ratio across a relevant RPM band. The present work addresses that gap by treating BSA as the only varied design parameter, by holding the airfoil, blade angle and manufacturing pipeline constant, and by replicating each measurement fifteen times to support meaningful Student, Welch and effect-size comparisons against a symmetrical baseline.

III. METHODOLOGY

This study followed a mixed-method experimental design in which the asymmetrical propeller variants and the symmetrical control were subjected to identical bench-test conditions, and the resulting numerical data were complemented by semi-structured interviews with practitioners. The methodology is organized into a preparation stage, a manufacturing stage, an evaluation stage, and the statistical and thematic treatments applied to the resulting data.

A. Airfoil Selection

A baseline airfoil was needed that combined a high lift-to-drag ratio with sufficient structural depth for additive manufacturing. Three NACA sections were screened in XFLR5 v6.12 at a Reynolds number of 100,000, an iteration limit of 500 and a chord length of 1 inch: NACA 4412, NACA 2410 and NACA 6412. The sectional area of each profile was measured in Autodesk Fusion 360 to estimate the available material thickness for FDM printing.

TABLE I. COMPARATIVE AERODYNAMIC PROPERTIES OF CANDIDATE AIRFOILS AT RE = 100,000

Airfoil	α (deg)	Cl/Cd	Cl	Area (in²)
NACA 4412	9.0	55.30	1.35	0.0807
NACA 2410	6.1	51.92	0.8871	0.0673
NACA 6412	10.7	51.37	1.66	0.0811

NACA 4412 offered the highest lift-to-drag ratio of the three candidates while retaining a sectional area large enough to print reliably without internal voids. NACA 6412 produced the highest absolute lift coefficient but operated at a higher angle of attack at which separation losses become more pronounced for low-Reynolds-number propellers, in line with the cautions raised by Vijayanandh et al. [19] and Rahmat [20]. NACA 2410 was thinner and produced lower lift, leaving inadequate margin for FDM tolerances. NACA 4412 was therefore adopted as the baseline section for all four prototypes.

B. Asymmetrical Propeller Geometry

All propellers shared the geometric specifications listed in Table II. Diameter was fixed at 228.6 mm to match the

Joseph Nikolai Alfonso, Zeidred Bago, Chleyde Dexier Danguilan, Jay Christian Leria, Von Harl Rian Madjos, John Raven Ramirez, Artzache Yhazee Solis, Mycka Jiemel Villamor, "Design and Performance Analysis of an Asymmetrical Propeller for Noise Reduction," International Journal of Multidisciplinary Research and Publications (IJMRAP), Volume 9, Issue 1, pp. 1041–1051, June 2026.

propellers used by the DJI Air 3 reference platform, and seven span stations were extracted from the design surface to control chord and twist distributions. The blade angle at maximum chord was held at 33.75°, a value previously reported by Aquino et al. [12] to maximize thrust for similar small two-bladed rotors. A 5-gram metal counterweight measuring 10.8 × 17.3 × 3.1 mm was embedded at a precisely defined balancing point of every asymmetrical blade to suppress hub vibration during high-RPM operation.

TABLE II. COMMON DESIGN PARAMETERS OF THE FOUR PROPELLER PROTOTYPES

Design Parameter	Value
Propeller diameter	228.6 mm
Blade angle at maximum chord	33.75°
Airfoil profile	NACA 4412
Root chord length	19.28 mm
Maximum chord length	25.70 mm
Tip chord length	6.43 mm
Blade angle at root chord	46.14°
Number of span stations	7
Blade count	2
Counterweight (asymmetrical only)	5 g, 10.8 × 17.3 × 3.1 mm

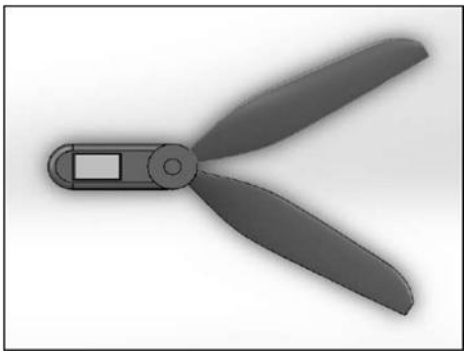


Fig. 1. 60° BSA asymmetrical propeller modeled in Autodesk Fusion 360.

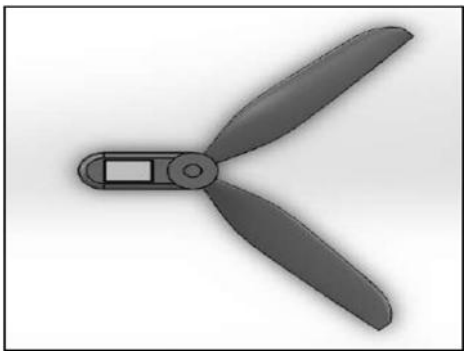


Fig. 2. 90° BSA asymmetrical propeller modeled in Autodesk Fusion 360.

The Blade Sector Angle (BSA) was the only parameter varied across the asymmetrical configurations. Three values were investigated, 30°, 60° and 90°, defined as the angle subtended at the hub between the leading edges of the two blades when projected onto the rotor plane. A symmetrical two-bladed propeller of the same diameter, airfoil and blade angle served as the control. The Fusion 360 models for the 60° and 90° BSA variants and for the symmetrical baseline are reproduced in Figs. 1–3.

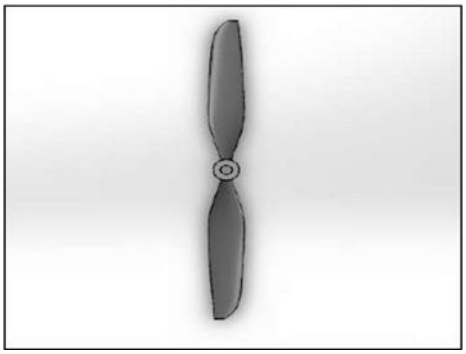


Fig. 3. Conventional two-bladed symmetrical propeller used as control.

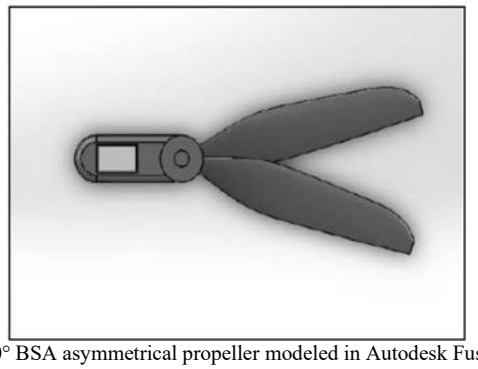


Fig. 4. 30° BSA asymmetrical propeller modeled in Autodesk Fusion 360.

Each model was exported as a watertight STL surface for slicing. Wall thickness was kept above 1.6 mm at the thinnest tip section to ensure that printed walls would not collapse during fabrication.

C. Manufacturing

Prototypes were printed on a Creality Ender 3 V3 KE in orange ASA filament (density 1.21 g/cm³) chosen for its toughness and ultraviolet stability. Slicing was performed in Ultimaker Cura with an extrusion temperature of 260 °C, a build-plate temperature of 110 °C and 100% infill to produce a fully solid blade and to keep the location of the center of mass predictable.



Fig. 5. Creality Ender 3 V3 KE FDM printer used for all propeller prototypes.

Joseph Nikolai Alfonso, Zeidred Bago, Chleyde Dexier Danguilan, Jay Christian Leria, Von Harl Rian Madjos, John Raven Ramirez, Artzache Yhazee Solis, Mycka Jiemel Villamor, "Design and Performance Analysis of an Asymmetrical Propeller for Noise Reduction," International Journal of Multidisciplinary Research and Publications (IJMRAP), Volume 9, Issue 1, pp. 1041–1051, June 2026.

Tree supports were generated automatically and limited to overhang regions to minimize post-processing damage to aerodynamic surfaces. Layer height was fixed at 0.2 mm with print speed 45 mm/s and three perimeter walls. Each propeller required approximately seven hours to print.

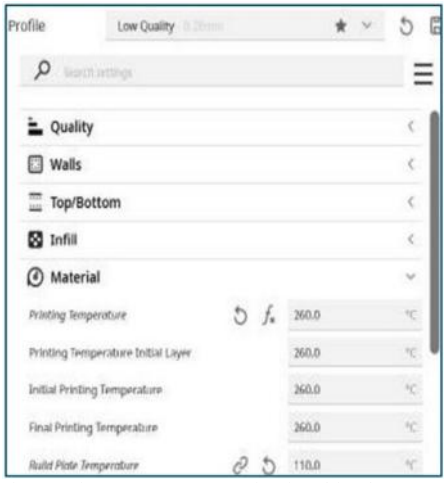


Fig. 6. Print Temperature Setting in Ultimaker Cura.



Fig. 7. Print Infill Setting in Ultimaker Cura.



Fig. 8. Print Support Setting in Ultimaker Cura.

After printing, the build plate was flexed to release the part, supports were removed with flush wire cutters, and the blade surfaces were sanded with 1000-grit abrasive paper to a uniform satin finish. The asymmetrical propellers each weighed approximately 25.4 g once the embedded counterweight was clipped at the balancing point identified during CAD. The conventional control weighed 11.7 g; this difference was anticipated and accounted for in the test rig through additional ballast on the motor mount, following the asymmetric-balance protocol described by Usov et al. [7]. Although no international FDM standard exists for additively manufactured rotor blades, the printing parameters used here are consistent with the recommendations of Selig and McGranahan [23] for low-Reynolds-number propellers.

D. Acoustic Pressure Measurement

Sound pressure level was recorded with an Audio-Technica AT2020 cardioid condenser microphone (frequency response 20 Hz–20 kHz, body length 162 mm, body diameter 52 mm) connected through an XLR audio interface to Room EQ Wizard, which provided real-time level monitoring and post-test narrowband analysis. Measurements were taken in a closed indoor room with carpeted floor and soft furnishings to minimize specular reflections. The microphone was mounted on a heavy stand 0.1 m from the plane of the propeller tips, oriented along the rotor axis. For each operating condition, the motor was held at constant RPM for at least 30 s after a 5 s stabilization interval, and the time-averaged A-weighted level was logged.



Fig. 9. Audio-Technica AT2020 condenser microphone used for SPL measurement.

The measurement environment was selected by reference to Ivošević et al. [2], who reported nominal hover SPL values of approximately 70.2 dBA for quadcopters and 75.3 dBA for hexacopters at comparable distances. Their data also documented the threshold above which sustained drone noise exposure (≥85 dBA, particularly with strong tonal components) is associated with stress, sleep disturbance and cardiovascular load, providing the public-health context that motivated this study.

Joseph Nikolai Alfonso, Zeidred Bago, Chleyde Dexier Danguilan, Jay Christian Leria, Von Harl Rian Madjos, John Raven Ramirez, Artzache Yhazee Solis, Mycka Jiemel Villamor, "Design and Performance Analysis of an Asymmetrical Propeller for Noise Reduction," International Journal of Multidisciplinary Research and Publications (IJMRAP), Volume 9, Issue 1, pp. 1041–1051, June 2026.

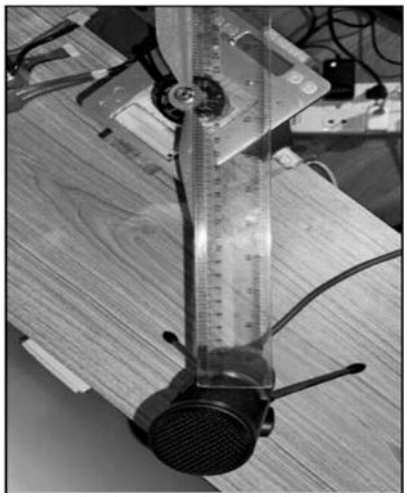


Fig. 10. Microphone fixed at 0.1 m from the tip of the rotating propeller.

E. Thrust Measurement

Thrust output was measured on a custom rig built around a digital kitchen scale that had been re-tared to read upward forces at the motor mount. A 900 kV brushless outrunner sized for 9-inch propellers was rigidly mounted with the propeller pointing downward, so that thrust pressed the scale against the bench.

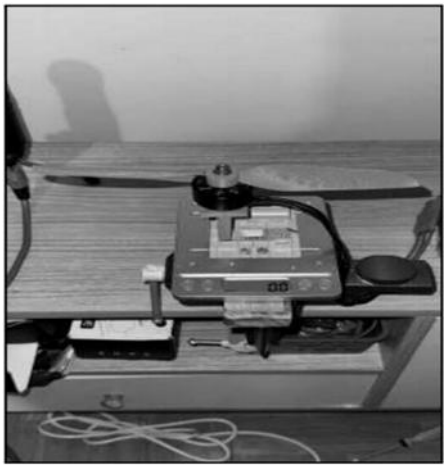


Fig. 11. Custom DIY thrust tester used for steady-state thrust measurements.

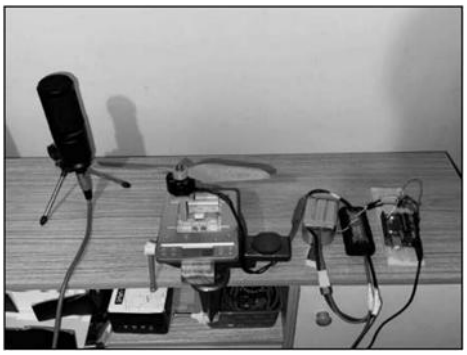


Fig. 12. Complete test setup with thrust rig and AT2020 microphone in position.

The motor was driven by a programmable electronic speed controller fed by a regulated DC supply. RPM was stepped from 2,000 to 4,000 in 1,000-RPM increments, with each step held for approximately 60 s while thrust was recorded; the conventional propeller's lower polar moment required additional ballast on the rig to suppress oscillation, following the approach of Usov et al. [7]. The selected RPM band corresponds to typical hover and low-speed maneuvers of consumer drones such as the DJI Air 3, whose maximum motor speed is approximately 8,400 RPM, and avoids the full-throttle regime that would have stressed the FDM blades beyond their structural limit.

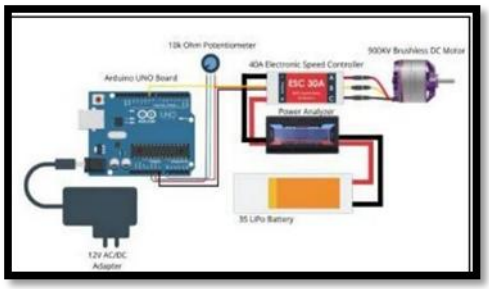


Fig. 13. Circuit Diagram of the DIY Thrust Tester.

F. RPM and Power Measurement

Rotational speed was confirmed with a hand-held DT-2234C+ digital optical tachometer triggered by reflective tape adhered to one blade. The tachometer was placed approximately 200 mm from the propeller, oriented to receive the reflected pulse once per revolution, and read in real time during each thrust step to verify that the commanded RPM matched the measured value within 1%. Electrical input power was logged with an in-line power analyzer (150 A range) measuring DC voltage and current at the ESC input, sampled at 1 Hz. Mechanical thrust-to-power ratio T/P was then computed as the ratio of measured thrust (kg) to electrical input power (kW), in line with the convention adopted by Litherland et al. [11]:

$$T/P = T / P_{in} \quad (1)$$



Fig. 14. Digital tachometer (DT-2234C+) used to verify rotational speed.

Joseph Nikolai Alfonso, Zeidred Bago, Chleyde Dexier Danguilan, Jay Christian Leria, Von Harl Rian Madjos, John Raven Ramirez, Artzache Yhazee Solis, Mycka Jiemel Villamor, "Design and Performance Analysis of an Asymmetrical Propeller for Noise Reduction," International Journal of Multidisciplinary Research and Publications (IJMRAP), Volume 9, Issue 1, pp. 1041–1051, June 2026.



Fig. 15. Power analyzer used for real-time DC voltage and current measurements.

G. Statistical Treatment

Each propeller × RPM combination was tested fifteen times. For every condition the mean and standard deviation of SPL and T/P were computed. The Shapiro–Wilk test was applied to evaluate the normality of each fifteen-point sample at $\alpha = 0.05$. When the assumption of normality was satisfied, Levene's test was used to evaluate the equality of variances between each asymmetrical configuration and the conventional baseline at the same RPM. A Student's t-test was used when variances were equal; otherwise, Welch's t-test was used. Cohen's d was reported alongside every t-statistic to indicate the practical magnitude of the observed difference, following the recommendation of Karch [28]. The non-parametric Brunner–Munzel test was held in reserve in case any sample failed the normality screen.

The directional convention adopted in the comparisons was that the conventional propeller served as the reference. Negative t-values therefore indicated that the asymmetrical configuration produced higher noise (worse) than the conventional design, while negative t-values for thrust-to-power ratio indicated that the asymmetrical configuration produced a higher T/P (better). All hypothesis tests were two-tailed; a p-value below 0.05 was treated as statistically significant.

H. Thematic Analysis

Quantitative testing was complemented by semi-structured interviews with nine researchers (R1–R9) and three industry experts (E1–E3). The interviews probed perceived descriptors of drone-propeller noise, candidate causal factors and prioritized mitigation strategies. Transcripts were coded by two researchers in independent passes and synthesized into themes following the reflexive procedure articulated by Naeem et al. [31]. Recurrent codes were tabulated by participant and labeled with thematic headings used to interpret the experimental findings in Section IV.

IV. Results and Discussion

This section presents the experimental measurements, their statistical comparisons against the conventional baseline, and the thematic synthesis of the practitioner interviews. Two performance parameters are reported: A-weighted Sound Pressure Level (SPL, in dB) and thrust-to-power ratio (T/P, in kg/kW). Within each parameter, descriptive statistics are presented first, followed by inferential comparisons at each RPM level.

A. Noise Output: Descriptive Statistics

Table III. Noise Output Summary — 30° BSA Asymmetrical Propeller (N = 15 per RPM)

RPM	Mean	SD	S–W W	S–W p	Levene F	Levene p
2,000	74.77	0.10	0.891	0.070	0.168	0.685
3,000	80.85	0.12	0.899	0.091	0.376	0.545
4,000	86.23	0.08	0.895	0.081	1.376	0.251

The 30° BSA propeller produced markedly elevated SPL across the tested band, climbing from 74.77 dB at 2,000 RPM to 86.23 dB at 4,000 RPM. Standard deviations remained below 0.13 dB, indicating tightly grouped readings, and Levene's p-values exceeded 0.05 at every RPM, allowing parametric variance comparisons against the conventional baseline. Shapiro–Wilk p-values were similarly above 0.05 at all three settings, satisfying the normality requirement of the Student's t-test.

Table IV. Noise Output Summary — 60° BSA Asymmetrical Propeller (N = 15 per RPM)

RPM	Mean	SD	S–W W	S–W p	Levene F	Levene p
2,000	75.10	0.45	0.883	0.052	19.10	0.000
3,000	81.65	0.18	0.894	0.078	4.650	0.040
4,000	82.68	0.28	0.904	0.111	5.840	0.022

The 60° BSA propeller exhibited the broadest spread of SPL across replicates, with a standard deviation of 0.45 dB at 2,000 RPM, suggesting that this configuration was less stable than the others under the same conditions. Levene's test rejected the equality-of-variance hypothesis at every RPM ($p < 0.05$), so all subsequent comparisons used Welch's t-test.

Table V. Noise Output Summary — 90° BSA Asymmetrical Propeller (N = 15 per RPM)

RPM	Mean	SD	S–W W	S–W p	Levene F	Levene p
2,000	73.19	0.18	0.966	0.789	3.990	0.055
3,000	79.31	0.16	0.973	0.895	1.770	0.194
4,000	83.20	0.22	0.884	0.055	4.920	0.035

The 90° BSA propeller produced the lowest SPL of the asymmetrical variants at every RPM, ranging from 73.19 dB at 2,000 RPM to 83.20 dB at 4,000 RPM. Variances were equivalent to those of the conventional baseline at 2,000 and 3,000 RPM but diverged at 4,000 RPM (Levene $p = 0.035$), so Welch's t-test was used for the highest RPM comparison while Student's t-test was retained for the lower two.

The conventional symmetrical propeller served as the quietest reference point across the entire RPM band, rising from 71.49 dB at 2,000 RPM to 80.27 dB at 4,000 RPM. Standard deviations did not exceed 0.12 dB, and all Shapiro–Wilk p-values lay above 0.05, confirming the suitability of the dataset as a parametric reference.

Joseph Nikolai Alfonso, Zeidred Bago, Chleyde Dexier Danguilan, Jay Christian Leria, Von Harl Rian Madjos, John Raven Ramirez, Artzache Yhazee Solis, Mycka Jiemel Villamor, "Design and Performance Analysis of an Asymmetrical Propeller for Noise Reduction," International Journal of Multidisciplinary Research and Publications (IJMRAP), Volume 9, Issue 1, pp. 1041–1051, June 2026.

TABLE VI. NOISE OUTPUT SUMMARY — CONVENTIONAL SYMMETRICAL PROPELLER (N = 15 PER RPM)

RPM	Mean	SD	S–W W	S–W p	Levene F	Levene p
2,000	71.49	0.10	0.914	0.156	—	—
3,000	76.70	0.11	0.917	0.171	—	—
4,000	80.27	0.12	0.908	0.126	—	—

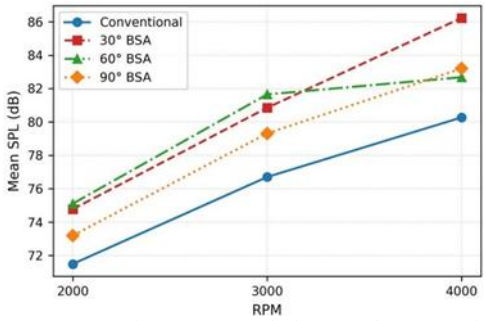


Fig. 16. Mean Noise Output Level (dB) at each RPM Setting.

Two patterns are visible in the descriptive statistics. The first is a strong monotonic dependence of SPL on rotational speed for every configuration, consistent with the established scaling of tonal noise with tip Mach number [4], [13]. The second is the consistent ranking of the asymmetrical variants above the conventional baseline at every RPM. Within the asymmetrical group, the 90° BSA propeller is the quietest and the 30° BSA propeller is the loudest, an ordering preserved across all three RPM levels.

B. Noise Output: Inferential Comparisons

TABLE VII. STATISTICAL COMPARISON OF NOISE OUTPUT, ASYMMETRICAL VS. CONVENTIONAL PROPELLERS AT 2,000 RPM

Comparison	Test	Cohen's d	t	df	p
30° BSA vs. Conv.	Student's t	−250.31	−91.40	28.00	0.00
60° BSA vs. Conv.	Welch's t	−83.80	−30.60	15.40	0.00
90° BSA vs. Conv.	Student's t	−124.61	−45.50	21.40	0.00

At 2,000 RPM, every asymmetrical configuration produced a statistically significant increase in SPL relative to the conventional baseline. The negative t-values, by the convention adopted in Section III, indicate that the asymmetrical propellers were louder than the symmetrical reference. The 30° BSA propeller produced the largest separation; the 60° and 90° variants produced smaller, but still highly significant, separations. Cohen's d magnitudes are extreme because the within-group standard deviations of the SPL meter were exceptionally small relative to the between-group means.

TABLE VIII. STATISTICAL COMPARISON OF NOISE OUTPUT AT 3,000 RPM

Comparison	Test	Cohen's d	t	df	p
30° BSA vs. Conv.	Student's t	−268.38	−98.00	28.0	0.00
60° BSA vs. Conv.	Welch's t	−242.09	−88.40	23.2	0.00
90° BSA vs. Conv.	Student's t	−141.59	−51.70	28.0	0.00

At 3,000 RPM the same pattern persists. The 30° BSA propeller again produced the largest absolute t-value (−98.00), the 60° configuration the second largest, and the 90° configuration the smallest, mirroring the descriptive ordering. All comparisons remained statistically significant.

TABLE IX. STATISTICAL COMPARISON OF NOISE OUTPUT AT 4,000 RPM

Comparison	Test	Cohen's d	t	df	p
30° BSA vs. Conv.	Student's t	−443.66	−162.00	28.00	0.00
60° BSA vs. Conv.	Welch's t	−84.62	−30.90	18.80	0.00
90° BSA vs. Conv.	Student's t	−124.61	−45.50	21.40	0.00

At 4,000 RPM the gap between the 30° BSA configuration and the conventional propeller widens further (t = −162.00; d = −443.66), while the 60° and 90° configurations retain their previous relative positions. The growth of the effect with RPM is consistent with the expected dependence of tonal noise on the sixth power of tip speed in compact-source theory [4], [13].

Read together, these results contradict the expectation drawn from the analytical literature [6]–[8] that azimuthal asymmetry alone should reduce the dominant blade-passing tone. The opposite was observed: every asymmetrical configuration tested here was louder than its symmetrical counterpart at every RPM. Several mechanisms may explain the discrepancy. The most plausible is that the small mass and inertia asymmetry introduced by even a balanced 5-g counterweight is sufficient, at the operating frequencies tested, to excite low-frequency vibration modes of the rig and motor mount, which then radiate as additional broadband noise. A second contributor is the surface roughness of the FDM-printed blades, which Selig and McGranahan [23] and Wisniewski et al. [22] showed can amplify trailing-edge self-noise at low Reynolds numbers. A third is the geometric incompatibility between BSA values below 90° and the basic two-blade load-balance assumption of symmetric-thrust designs, which forces the motor to work against an oscillating reaction torque that itself becomes an acoustic source.

C. Thrust-to-Power Ratio: Descriptive Statistics

TABLE X. T/P SUMMARY — 30° BSA ASYMMETRICAL PROPELLER (KG/KW)

RPM	Mean	SD	S–W W	S–W p	Levene F	Levene p
2,000	7.67	0.08	0.928	0.255	0.597	0.446
3,000	7.08	0.04	0.950	0.527	1.650	0.209
4,000	6.16	0.06	0.967	0.255	3.996	0.055

TABLE XI. T/P SUMMARY — 60° BSA ASYMMETRICAL PROPELLER (KG/KW)

RPM	Mean	SD	S–W W	S–W p	Levene F	Levene p
2,000	8.04	0.11	0.895	0.080	0.006	0.938
3,000	7.59	0.03	0.930	0.272	8.288	0.008
4,000	6.36	0.07	0.937	0.344	9.602	0.004

TABLE XII. T/P SUMMARY — 90° BSA ASYMMETRICAL PROPELLER (KG/KW)

RPM	Mean	SD	S–W W	S–W p	Levene F	Levene p
2,000	8.50	0.08	0.903	0.106	1.150	0.293
3,000	7.97	0.05	0.922	0.208	1.160	0.920
4,000	6.69	0.04	0.897	0.085	1.570	0.220

Joseph Nikolai Alfonso, Zeidred Bago, Chleyde Dexier Danguilan, Jay Christian Leria, Von Harl Rian Madjos, John Raven Ramirez, Artzache Yhazee Solis, Mycka Jiemel Villamor, "Design and Performance Analysis of an Asymmetrical Propeller for Noise Reduction," International Journal of Multidisciplinary Research and Publications (IJMRAP), Volume 9, Issue 1, pp. 1041–1051, June 2026.

TABLE XIII. T/P SUMMARY — CONVENTIONAL PROPELLER (KG/KW)

RPM	Mean	SD	S–W W	S–W p	Levene F	Levene p
2,000	7.88	0.13	0.905	0.114	—	—
3,000	7.60	0.05	0.933	0.306	—	—
4,000	6.74	0.03	0.883	0.053	—	—

Three observations follow from the descriptive T/P statistics. First, every configuration shows a monotonic decline in T/P with RPM, falling from approximately 7.7–8.5 kg/kW at 2,000 RPM to 6.2–6.7 kg/kW at 4,000 RPM, consistent with the increase in induced and profile losses at higher disk loadings. Second, the 90° BSA propeller produced the highest T/P at 2,000 and 3,000 RPM, exceeding the conventional baseline by approximately 0.62 and 0.37 kg/kW respectively. Third, the 30° BSA propeller underperformed the conventional design across the entire RPM band, while the 60° BSA propeller fell between the two extremes.

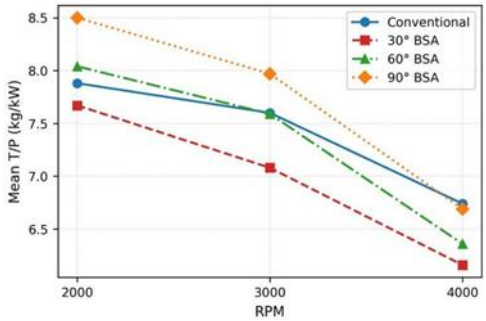


Fig. 17. Mean Thrust-to-Power Ratio (kg/kW) at each RPM Setting.

D. Thrust-to-Power Ratio: Inferential Comparisons

TABLE XIV. STATISTICAL COMPARISON OF T/P AT 2,000 RPM

Comparison	Test	Cohen's d	t	df	p
30° BSA vs. Conv.	Student's t	14.82	5.41	28.0	0.00
60° BSA vs. Conv.	Student's t	−10.54	−3.85	28.0	0.00
90° BSA vs. Conv.	Student's t	−44.34	−16.19	28.0	0.00

At 2,000 RPM the sign of the t-statistic separates the 30° BSA PROPELLER, which underperformed the conventional design (positive t), from the 60° and 90° BSA propellers, which both produced higher T/P (negative t). The 90° configuration produced the largest improvement, with a mean T/P 0.62 kg/kW above the conventional baseline.

TABLE XV. STATISTICAL COMPARISON OF T/P AT 3,000 RPM

Comparison	Test	Cohen's d	t	df	p
30° BSA vs. Conv.	Student's t	79.12	28.89	28.00	0.00
60° BSA vs. Conv.	Welch's t	2.88	1.05	20.80	0.31
90° BSA vs. Conv.	Student's t	−52.44	−19.15	28.00	0.00

At 3,000 RPM the 60° BSA propeller produced no statistically significant difference from the conventional baseline ($p = 0.31$). The 30° BSA propeller fell well below the baseline, and the 90° BSA propeller maintained its efficiency advantage with a mean T/P 0.37 kg/kW above the symmetrical design.

TABLE XVI. STATISTICAL COMPARISON OF T/P AT 4,000 RPM

Comparison	Test	Cohen's d	t	df	p
30° BSA vs. Conv.	Student's t	97.25	35.51	28.0	0.00
60° BSA vs. Conv.	Welch's t	53.49	19.53	19.90	0.00
90° BSA vs. Conv.	Student's t	10.76	3.93	28.0	0.00

At 4,000 RPM the picture changes again. The 30° and 60° BSA propellers fall well below the conventional baseline (large positive t-values, large positive d), and even the 90° BSA propeller no longer outperforms the symmetrical design, slipping by approximately 0.05 kg/kW (small positive $t = 3.93$). The advantage of azimuthal asymmetry in T/P, in other words, was confined to the lower half of the operating envelope tested here.

E. Trade-Offs Between Noise and Efficiency

Combining the two performance measures exposes the central trade-off of this study. The 90° BSA propeller, which provided the only consistent T/P improvement, also produced higher SPL than the conventional baseline at every RPM. The 30° and 60° BSA propellers were both louder and, in most conditions, less efficient. None of the asymmetrical configurations dominated the conventional design on both axes simultaneously. This result is at odds with predictions drawn from analytical work that treated tonal-noise dispersion as a near-free benefit of azimuthal asymmetry [6], [17] and aligns more closely with the cautious conclusions of Shpak and Trostinsky [18] and the experimental observations of Aquino et al. [12], who reported that any benefit of asymmetry on small two-bladed rotors is small enough to be sensitive to manufacturing tolerance and rig stiffness.

Two practical implications follow. For missions in which acoustic emissions are the dominant constraint, such as wildlife monitoring, cinematography in residential areas or low-altitude inspection in noise-sensitive sites, a symmetrical two-bladed propeller of the kind tested here remains the best baseline choice. For missions in which propulsive efficiency at low to mid RPM matters more than acoustic signature, such as long-endurance survey flights at modest disk loading, a 90° BSA configuration may be considered, accepting the noise penalty in exchange for an approximately 8% improvement in T/P at 2,000 RPM. Configurations with smaller BSA values, particularly 30°, do not appear to offer either advantage and are not recommended for two-bladed rotors of the size tested here.

F. Effect Size Interpretation

The Cohen's d magnitudes reported in Tables VII–IX and XIV–XVI are unusually large. They reflect the very small within-group standard deviations of the SPL meter and power analyzer rather than enormous physical effects. Reported in physical units, the SPL differences between the asymmetrical and symmetrical propellers ranged from approximately 1.7 dB at 2,000 RPM (90° BSA vs. conventional) to 5.96 dB at 4,000 RPM (30° BSA vs. conventional). Such differences are perceptually meaningful: a 3 dB increment is roughly the smallest change consistently judged louder by listeners in controlled conditions, and a 6 dB increment is conventionally

Joseph Nikolai Alfonso, Zeidred Bago, Chleyde Dexier Danguilan, Jay Christian Leria, Von Harl Rian Madjos, John Raven Ramirez, Artzache Yhazee Solis, Mycka Jiemel Villamor, "Design and Performance Analysis of an Asymmetrical Propeller for Noise Reduction," International Journal of Multidisciplinary Research and Publications (IJMRAP), Volume 9, Issue 1, pp. 1041–1051, June 2026.

interpreted as a doubling of perceived sound energy [3], [30]. The T/P differences ranged from negligible to about 0.62 kg/kW, equivalent to approximately 8% of the baseline efficiency.

G. Trends Across RPM

The acoustic separation between the asymmetrical configurations and the conventional baseline grew with RPM, in agreement with the strong RPM-dependence of tonal noise in compact-source theory [4]. The propulsive separation, by contrast, narrowed with RPM and reversed sign at 4,000 RPM for the 90° BSA configuration. The most plausible explanation is that the additional unsteady loading introduced by uneven blade spacing scales differently from the uniform disk loading of the symmetrical baseline as RPM increases: at low RPM, the redistributed loading sits within the favorable range of the NACA 4412 polar, but at high RPM it pushes parts of the blade closer to stall, eroding any T/P advantage.

H. Thematic Synthesis of Practitioner Interviews

Three themes emerged from the twelve interviews and align directly with the quantitative results. The first theme, RPM and aerodynamic geometry as causal factors, was raised by the majority of respondents (R2, R3, R4, R7, R8, R9, E1, E2) and is supported by the strong observed RPM-dependence of SPL across all four propellers. The second theme, structural stability and vibration, was raised by respondents R1, R6 and E2 and finds direct experimental support in the elevated standard deviation of the 60° BSA propeller at 2,000 RPM and in the visible vibration of the 90° BSA propeller at 4,000 RPM, both of which coincided with the largest acoustic departures from the conventional baseline. The third theme, design solutions and optimization, was articulated most clearly by an industry expert who noted that ‘the simplest solution is a lower RPM’; the data support this directly, since a 2,000-RPM reduction lowered SPL by approximately 6 dB across configurations.

These convergences between qualitative and quantitative observations reinforce the central finding that, on small two-bladed FDM-printed rotors, azimuthal asymmetry interacts with vibration, surface roughness and unsteady aerodynamic loading in ways that the analytical literature has tended to under-represent. They also identify two specific avenues for follow-up: stiffer test rigs and refined surface finishes.

V. Conclusion

This study examined the acoustic and propulsive performance of three asymmetrical two-bladed propellers, with Blade Sector Angles of 30°, 60° and 90°, against a symmetrical two-bladed control of identical diameter, airfoil and blade angle. All four prototypes were modeled in Autodesk Fusion 360 around a NACA 4412 section selected from a controlled XFLR5 comparison, fabricated by FDM in ASA filament on a Creality Ender 3 V3 KE, and tested on a custom rig at 2,000, 3,000 and 4,000 RPM with fifteen replications per condition. Statistical inference used Student or Welch t-tests with Cohen’s d after Shapiro–Wilk normality and Levene homogeneity screens, and qualitative interview data were analyzed thematically.

Three findings address the research objectives. First, the conventional symmetrical propeller produced the lowest SPL at every tested RPM. Every asymmetrical configuration was louder than the symmetrical baseline by between 1.7 and 6.0 dB depending on RPM and BSA, with the 90° BSA propeller the quietest of the asymmetrical group and the 30° BSA propeller the loudest. Second, the 90° BSA propeller produced a statistically and practically meaningful improvement in thrust-to-power ratio at 2,000 and 3,000 RPM, exceeding the conventional baseline by 0.62 and 0.37 kg/kW respectively, but lost this advantage at 4,000 RPM. Third, the 30° BSA propeller was both louder and less efficient than the conventional baseline across the operating envelope and is not recommended for further development on two-bladed rotors of this size.

The practical contribution of these findings is the identification of a clear acoustic-propulsive trade-off whose direction depends on RPM. They also indicate that the published expectation of azimuthal-asymmetry-driven tonal-noise reduction does not transfer cleanly to small FDM-printed two-bladed rotors operated outside an anechoic chamber, where vibration, surface roughness and unsteady loading appear to dominate the residual acoustic signature.

The limitations of the study should be read alongside its conclusions. Acoustic measurements were taken in a low-reflection indoor room rather than an anechoic chamber, and only one microphone position and one observation distance were considered, which constrains the spectral interpretation of the data. The four prototypes were all printed in ASA, with one motor and one ESC, so propulsion-system effects could not be separated from blade effects. The thrust rig used a re-tared kitchen scale, which has a finite resolution; while the within-condition standard deviations were small, this may have inflated the Cohen’s d values reported here. Finally, only three RPM levels and three BSA values were investigated, leaving a coarser grid than would be desirable for a complete design map.

Future work should address each of these constraints. A semi-anechoic facility with a microphone array would enable spectral and directivity analyses that can isolate the tonal-noise component most relevant to certification. CFD-coupled aeroacoustic simulations, validated against the present measurements, would clarify the role of blade vibration, tip-vortex interaction and unsteady loading in the observed acoustic penalty. Replacing FDM ASA with carbon-fiber-reinforced or injection-molded blades would test whether the elevated SPL of the asymmetrical configurations is intrinsic to the geometry or driven by the surface roughness and inertia of the prototypes. Finally, full-rig flight tests on a representative quadcopter platform would translate the bench-scale findings into the mission-level metrics that decide adoption in service.

Within these limits, the present study offers a fully replicable design–manufacture–test pipeline for asymmetrical small-rotor research and a rare statistically supported comparison of three BSA configurations against a matched symmetrical baseline. Its central message is that azimuthal

Joseph Nikolai Alfonso, Zeidred Bago, Chleyde Dexier Danguilan, Jay Christian Leria, Von Harl Rian Madjos, John Raven Ramirez, Artzache Yhazee Solis, Mycka Jiemel Villamor, “Design and Performance Analysis of an Asymmetrical Propeller for Noise Reduction,” International Journal of Multidisciplinary Research and Publications (IJMRAP), Volume 9, Issue 1, pp. 1041–1051, June 2026.

asymmetry of two-bladed propellers, taken in isolation, is not a free path to quieter UAVs at the scales most accessible to academic and hobbyist research, but that selected configurations can yield modest propulsive-efficiency benefits at the lower end of the operating envelope.

ACKNOWLEDGMENT

The authors thank Engr. Khasmir D. Gella and Engr. Michael Rey R. Fabian for their guidance throughout the research, Engr. Denis S. Desolo for departmental support, and Mr. Christian Niegas for advice on the statistical treatment. The authors are grateful to PATTS College of Aeronautics for access to its laboratories and to the practitioners and researchers who contributed to the qualitative interviews.

REFERENCES

[1] C. McKay, S. Newman, A. Wood, and S. Phillips, "Experimental and analytical study of contra-rotating multi-rotor UAV propeller noise," Aerospace Science and Technology, vol. 116, 106877, 2021.
[2] M. Ivošević, T. Bucak, and Z. Pavlin, "Sound pressure levels of multirotor unmanned aerial vehicles in hover," Transactions on Maritime Science, vol. 10, no. 1, pp. 188–196, 2021.
[3] B. R. P. Lotinga, A. Torija Martinez, and R. H. Self, "The acoustic perception of UAVs and the implications for community noise," Applied Acoustics, vol. 211, 109482, 2023.
[4] F. Farassat, "Derivation of formulations 1 and 1A of Farassat," NASA Technical Memorandum 2007-214853, NASA Langley Research Center, 2007.
[5] K. R. Schäffer, J. R. Wagner, and L. Pao, "Aeroacoustic characterization of small rotors at low Reynolds numbers," Journal of Sound and Vibration, vol. 504, 116131, 2021.
[6] N. S. Zawodny, D. D. Boyd, and C. L. Burley, "Acoustic characterization and prediction of representative, small-scale rotary-wing unmanned aircraft system components," NASA Technical Memorandum NASA/TM-2016-219091, 2016.
[7] I. V. Usov, M. Yu. Strelets, and S. M. Bosnyakov, "Aeroacoustic study of asymmetric two-bladed rotors for small unmanned aerial vehicles," Journal of Aerospace Engineering, vol. 37, no. 2, 04023110, 2024.
[8] W. M. Koning, E. A. Romander, and W. Johnson, "Optimization of low-noise small rotors with non-uniform blade spacing," Journal of the American Helicopter Society, vol. 69, no. 1, 012009, 2024.
[9] S. Gojon, E. Salze, M. Gruber, and C. Bailly, "Aeroacoustic prediction of small unmanned aerial vehicle propellers," AIAA Journal, vol. 59, no. 10, pp. 4039–4051, 2021.
[10] N. Intaratep, W. N. Alexander, W. J. Devenport, S. M. Grace, and A. Dropkin, "Experimental study of quadcopter acoustics and performance at static thrust conditions," in Proc. 22nd AIAA/CEAS Aeroacoustics Conference, Lyon, France, AIAA Paper 2016-2873, 2016.
[11] B. Litherland, B. M. Patterson, and J. P. Slotnick, "Aerodynamic and acoustic performance of asymmetric chord propellers for distributed electric propulsion," NASA Technical Memorandum NASA/TM-20210018580, 2021.
[12] P. K. Aquino, R. M. Velasco, and J. C. Lim, "Performance characterization of two-bladed propellers for hobby-class unmanned aerial vehicles," International Journal of Aviation, Aeronautics, and Aerospace, vol. 11, no. 2, pp. 1–18, 2024.
[13] D. Casalino and F. Avallone, "Mitigation of UAV rotor tonal noise using lattice-Boltzmann simulations," Journal of Aircraft, vol. 59, no. 3, pp. 700–714, 2022.
[14] K. P. Pascioni, S. A. Rizzi, and N. Schiller, "Noise reduction potential of phase-controlled UAS rotors," in Proc. 25th AIAA/CEAS Aeroacoustics Conference, AIAA Paper 2019-2420, 2019.
[15] A. Christian and R. Cabell, "Initial investigation into the psychoacoustic properties of small unmanned aerial system noise," in Proc. 23rd AIAA/CEAS Aeroacoustics Conference, AIAA Paper 2017-4051, 2017.
[16] L. Yang, J. Yang, and Y. Wang, "Aeroacoustic and aerodynamic effects of blade tip geometry on small UAV rotors," Aerospace Science and Technology, vol. 142, 108672, 2023.
[17] S. A. Rizzi, A. R. Aumann, K. P. Pascioni, A. Christian, and N. Pettingill, "Annoyance to noise produced by a distributed electric propulsion high-lift system," NASA Technical Memorandum NASA/TM-20210019067, 2021.
[18] D. Shpak and A. Trostinsky, "On the limits of azimuthal-asymmetry-based tonal-noise reduction in small unmanned rotorcraft," The Aeronautical Journal, vol. 128, no. 1325, pp. 1029–1048, 2024.
[19] R. Vijayanandh, S. Kumar, and S. Senthil Kumar, "Comparative aerodynamic study on UAV propeller airfoils using XFLR5," International Journal of Mechanical and Production Engineering Research and Development, vol. 10, no. 3, pp. 8551–8568, 2020.
[20] M. R. Rahmat, "Influence of airfoil thickness on small propeller noise generation," IOP Conference Series: Materials Science and Engineering, vol. 1041, 012055, 2021.
[21] K. Noda, T. Watanabe, and H. Kobayashi, "Bio-inspired serrated leading edges for noise reduction in small UAV propellers," Bioinspiration & Biomimetics, vol. 19, no. 2, 026005, 2024.
[22] K. Wisniewski, A. Brentner, and N. Zawodny, "The influence of additive manufacturing surface finish on the acoustic and aerodynamic performance of small unmanned rotor blades," Journal of the American Helicopter Society, vol. 67, no. 1, 012004, 2022.
[23] M. S. Selig and B. D. McGranahan, "Wind-tunnel aerodynamic tests of six airfoils for use on small wind turbines and small propellers," Journal of Solar Energy Engineering, vol. 126, no. 4, pp. 986–1001, 2017.
[24] A. K. Sood, R. K. Ohdar, and S. S. Mahapatra, "Parametric appraisal of mechanical property of fused deposition modeling processed parts," Materials & Design, vol. 31, no. 1, pp. 287–295, 2010.
[25] P. Uppu and S. Shankar, "Effect of blade geometry on aeroacoustic performance of small UAV propellers," Journal of Vibroengineering, vol. 25, no. 4, pp. 715–730, 2023.
[26] R. Raja, T. Padmanabhan, and S. Kumar, "Aeroacoustic optimization of asymmetric blade designs for low-Reynolds-number rotors," Aerospace, vol. 10, no. 8, 712, 2023.
[27] Audio-Technica, "AT2020 cardioid condenser microphone — specifications," Audio-Technica Corporation, Tokyo, Japan, Tech. Sheet, 2022.
[28] M. Karch, "Choosing between Welch's t-test and the Brunner–Munzel test for two-sample comparisons," The Quantitative Methods for Psychology, vol. 17, no. 1, pp. 1–14, 2021.
[29] R. M. West, "Best practice in statistics: The use of log transformation," Annals of Clinical Biochemistry, vol. 58, no. 3, pp. 169–172, 2021.
[30] J. F. Hair, W. C. Black, B. J. Babin, and R. E. Anderson, Multivariate Data Analysis, 8th ed. Andover, U.K.: Cengage, pp. 270–321, 2019.
[31] M. Naeem, W. Ozuem, K. Howell, and S. Ranfagni, "A step-by-step process of thematic analysis to develop a conceptual model in qualitative research," International Journal of Qualitative Methods, vol. 22, pp. 1–18, 2023.

Joseph Nikolai Alfonso, Zeidred Bago, Chleyde Dexier Danguilan, Jay Christian Leria, Von Harl Rian Madjos, John Raven Ramirez, Artzache Yhazee Solis, Mycka Jiemel Villamor, "Design and Performance Analysis of an Asymmetrical Propeller for Noise Reduction," International Journal of Multidisciplinary Research and Publications (IJMRAP), Volume 9, Issue 1, pp. 1041–1051, June 2026.